

An Introduction to Molecular Imaging

Silvio Aime

Dipartimento di Chimica I.F.M., Università di Torino, Italy



Molecular Imaging

- In vivo characterization of and measurement of biological process at cellular and molecular level
- Probe the molecular abnormalities at the basis of disease rather than imaging the end effects of the molecular alterations
- Combine new molecular agents with traditional imaging tools to create targeted, tailored therapies with the ability to simultaneously find , diagnose and treat disease

The practice of Diagnostic Imaging in the era of Molecular Medicine

Molecular Imaging Applications

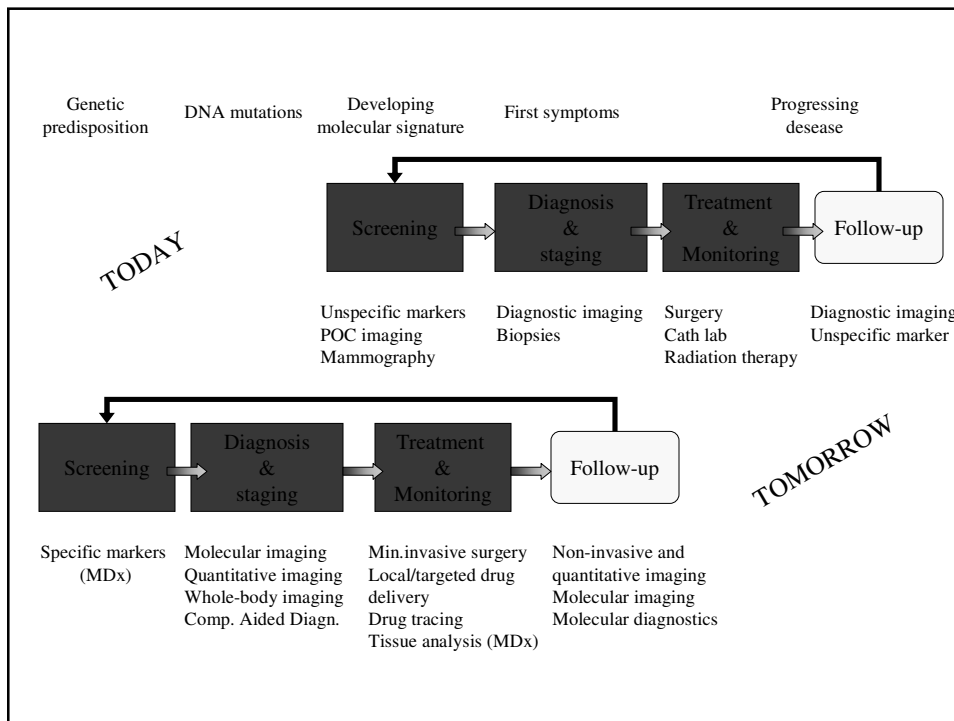
- Oncology
- Cardiology
- Neurology

Finding targeted cells

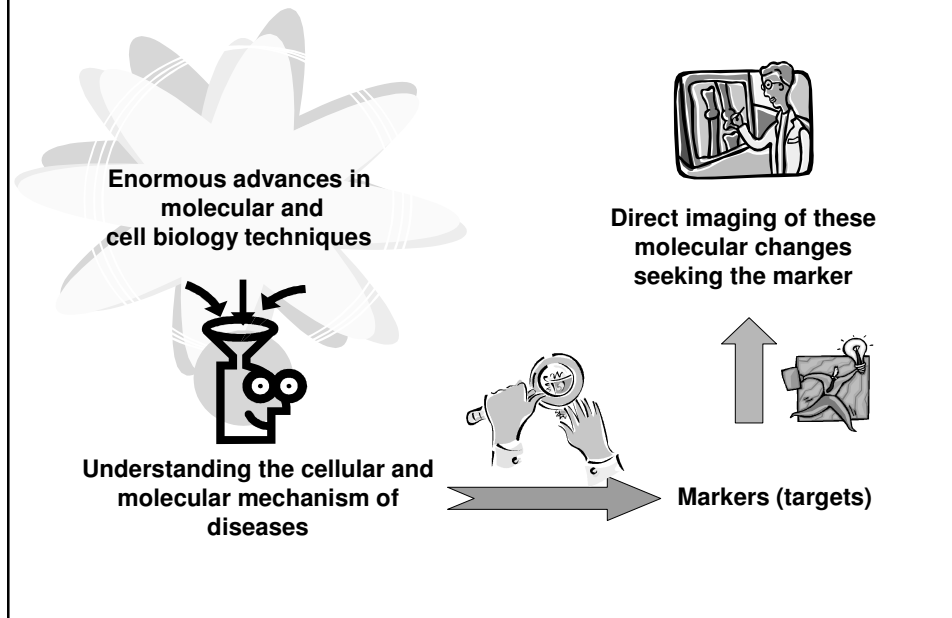
Identifying cell death

Assessing the efficacy of therapy

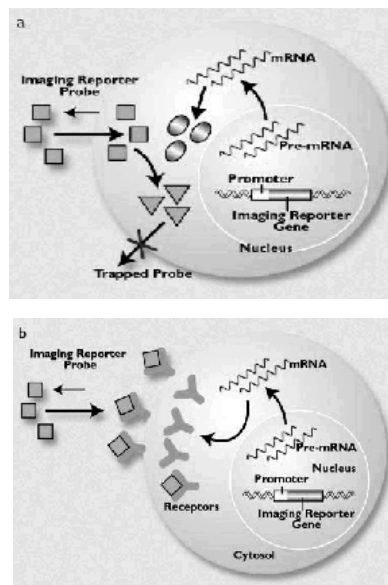
Delivering therapy to targeted cells



Molecular Imaging



Approach to imaging reporter genes



- a) The imaging reporter probe is trapped in intracellular enzymes, encoded by imaging reporter genes, requiring the probe to cross the cell membrane.
- b) The imaging reporter probe links to cell surface proteins or receptors, encoded by imaging reporter genes, so that it does not need to cross the cell membrane.

MEDICAMUNDI 47/1 APRIL 2003

Imaging Techniques

Nuclear Medicine (PET, SPECT)

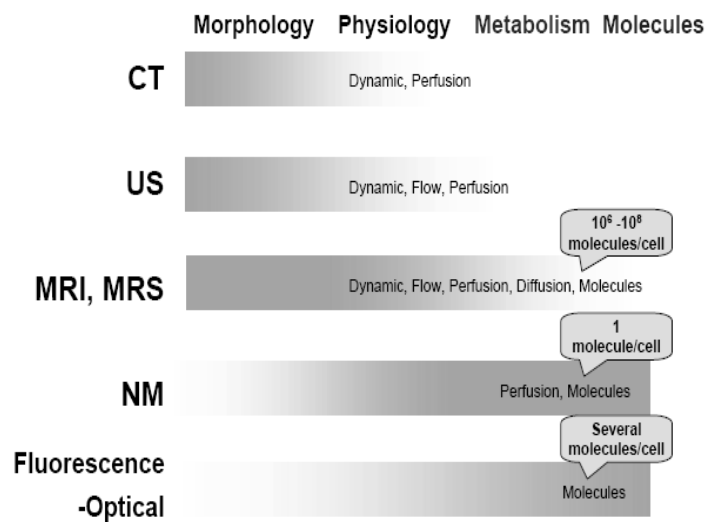
Magnetic Resonance (MRI)

Computed Tomography (CT)

Ultrasound

Optical Imaging

Imaging Modalities



Nuclear Medicine



Positron Emission Tomography

β^+ emitting isotopes



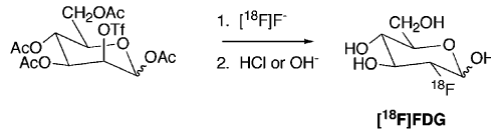
Single Photon Emission Computed Tomography

γ emitting isotopes

	Isotope	$T_{1/2}$ [h]	Decay Mode (%)	E [keV] (%)	Production Mode
β^+ -emitter	^{18}F	1.83	β^+ , EC	635 (97)	Cyclotron $^{18}\text{O}(p,n)^{18}\text{F}$
	^{124}I	76.8	β^+ , EC	790 1530 2130	
	^{64}Cu	12.9	β^+ (19.3) β^- (39.6) EC (45)	654(19) 573(40)	reactor, cyclotron
	^{68}Ga	1.14	β^+ (90) EC(10)	820 1865	$^{68}\text{Ge}/^{68}\text{Ga}$ generator
	^{86}Y	14.7	β^+ (33) EC(66)	1250(11) 1600(5) 2020(4) 2340(11)	Cyclotron $^{86}\text{Sr}(p,n)^{86}\text{Y}$

	Isotope	$T_{1/2}$ [h]	Decay Mode	E [keV] (%)	Production Mode
γ -emitter	$^{99\text{m}}\text{Tc}$	6.02	γ	141	$^{99}\text{Mo}/^{99\text{m}}\text{Tc}$ generator
	^{111}In	67.2	Auger, EC(100)	172(90) 247(94)	Cyclotron Cd(p,n) ^{111}In
	^{67}Ga	78.1	EC, Auger	93(38) 185(24) 300(16)	Cyclotron $^{68}\text{Zn}(p,2n)^{67}\text{Ga}$
	^{123}I	13.0	EC	159(84) 27(71)	Cyclotron $^{124}\text{Te}(p,2n)^{123}\text{I}$

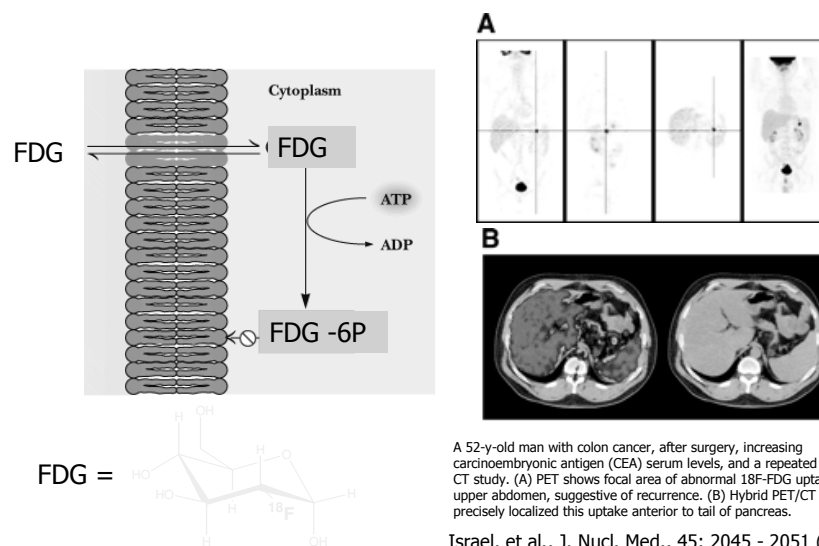
[¹⁸F]-FDG synthesis



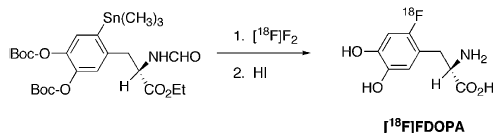
Radiofluorination of a glucose derivative by nucleophilic displacement reaction

Synthesis preparation time	Less than 5 minutes
Synthesis time	25 minutes
Production yield, not corrected for decay	Typical 60 %
Radiochemical yield, decay corrected	Typical 70 %
Residual activity at end of synthesis	< 0.5 %

In the world of PET, metabolic imaging means FDG!



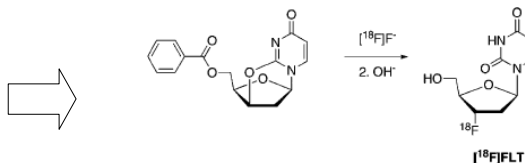
[¹⁸F]-DOPA and [¹⁸F]-FLT syntheses



Synthesis preparation time	< 15 min
Synthesis time	< 40 min
Production yield (not corrected for decay)	Typical 20 %
Radio chemical conversion yield (corrected for decay)	Typical 25 %
Enantiomeric purity	≥ 99 %

[¹⁸F]-DOPA is synthesised through an electrophilic destannylation reaction in less than 40 minutes

Another example of nucleophilic displacement



Imaging cell proliferation by PET

Shields, *et al.*, Nat Med, 4: 1334–1336 (1998)

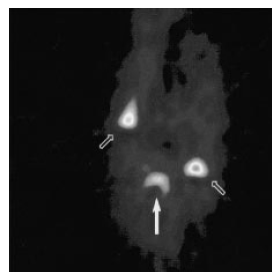
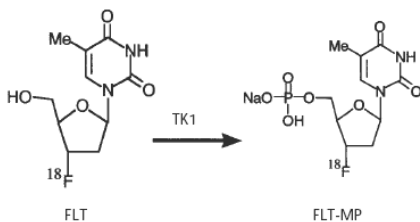


Fig. 1 Structure of FLT and its phosphorylation by thymidine kinase 1 (TK1). Replacement of the F in the FLT structure by OH = thymidine; N₃ = AZT.

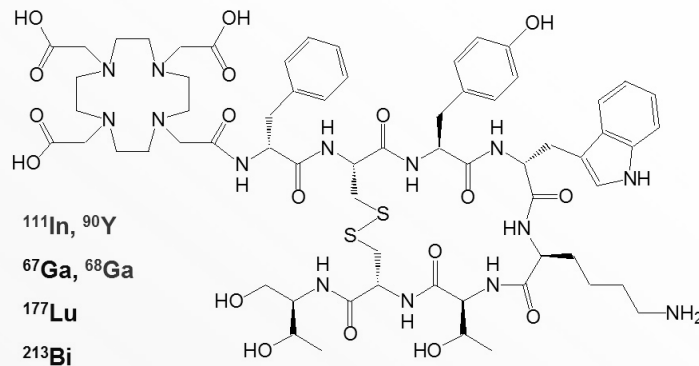
FLT image of the neck of a dog with non-Hodgkin's lymphoma in two enlarged nodes (open arrows) and marrow activity (filled arrow) as well. The image was obtained from 20–60 min post-injection.

^{68}Ga , an ideal metallic positron emitter!

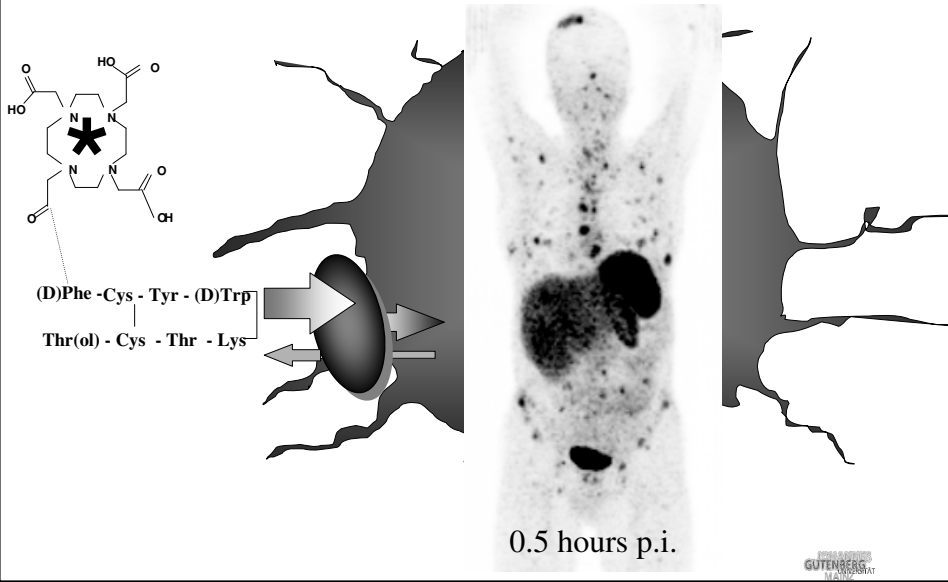
- ➔ Generator produced ($^{68}\text{Ge}/^{68}\text{Ga}$)
- ➔ high positron yield (90%)
- ➔ 68 min half-life
- ➔ parent ^{68}Ge : 270 d half-life
- ➔ established chemistry
- ➔ ^{68}Ga -DOTATOC, an ideal PET tracer to image neuroendocrine tumors?
- There is a need to develop more ^{68}Ga -based PET tracer

Structural Formula of DOTA-Tyr³-Octreotide

■ DOTA-TOC



^{68}Ga -DOTA-(D)Phe¹-Tyr³-octreotide and PET/CT



Nuclear Medicine



**Positron Emission
Tomography**

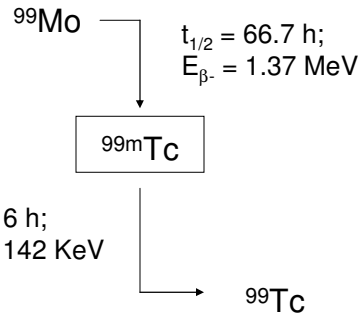
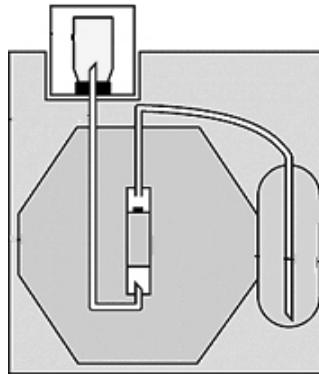
β^+ emitting isotopes



**Single Photon
Emission Computed
Tomography**

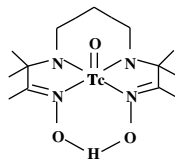
γ emitting isotopes

The $^{99}\text{Mo}/^{99\text{m}}\text{Tc}$ generator

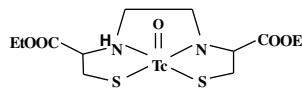


The separation of $^{99\text{m}}\text{Tc}$ from ^{99}Mo is accomplished by the selective elution of $^{99\text{m}}\text{TcO}_4^-$ with sterile saline from an alumina column containing $^{99}\text{MoO}_4^{2-}$.

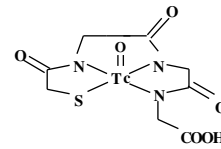
Clinically approved radiopharmaceuticals based on $^{99\text{m}}\text{Tc}$



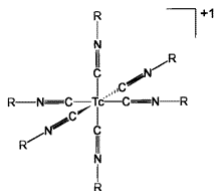
Tc(O)(HM-PAO)
® Ceretec



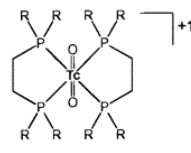
TcO(ECD)
® Neurolite



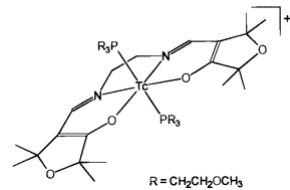
[TcO(MAG₃)]⁻
® Technescan



$^{99\text{m}}\text{Tc}$ -sestamibi
(Cardiolite)

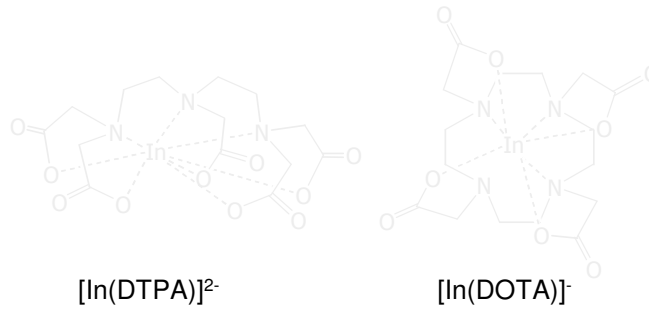


$^{99\text{m}}\text{Tc}$ -tetrofosmin
(Myoview)



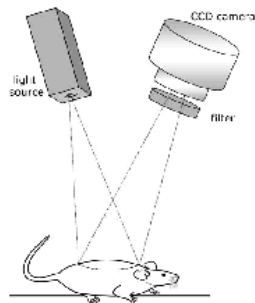
$^{99\text{m}}\text{Tc}$ -furifosmin
(Technescan Q12)

^{111}In complexes

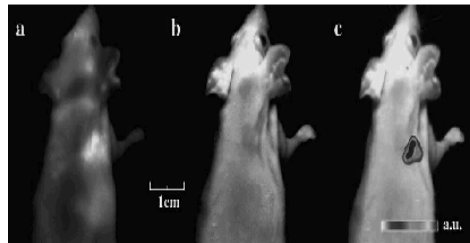


^{111}In -OCTREOSCAN is a DTPA conjugated to a somatostatin pentapeptide analogue used in clinics.

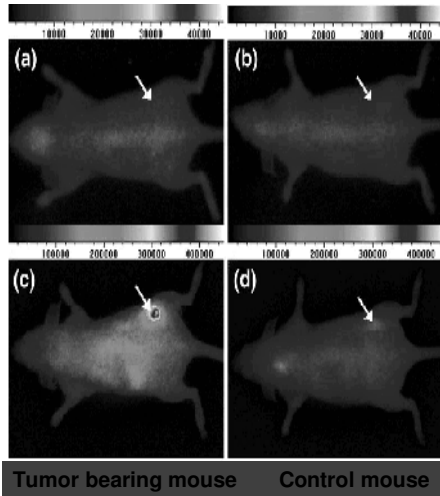
Optical Imaging



- In vivo system for fluorescence reflectance
- High sensitivity
- Drawbacks: penetration of light in biological tissues, autofluorescence
- Very useful in drug development
- The probe are dark in the native state and after enzymatic cleavage of the black-bone carrier they fluoresce when appropriately excited



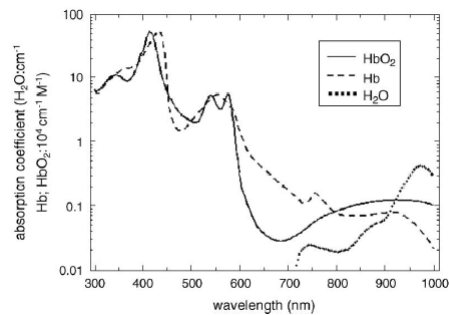
Optical Imaging



- Tumor bearing mice (RIN38 pancreatic tumor expressing somatostatin receptor)
- Somatostatin analog ocreotide coupled with indocarbocyanine dyes
- 0.02 $\mu\text{mol/kg}$ iv
- Enhanced tumor at 6h after injection

Optical Imaging

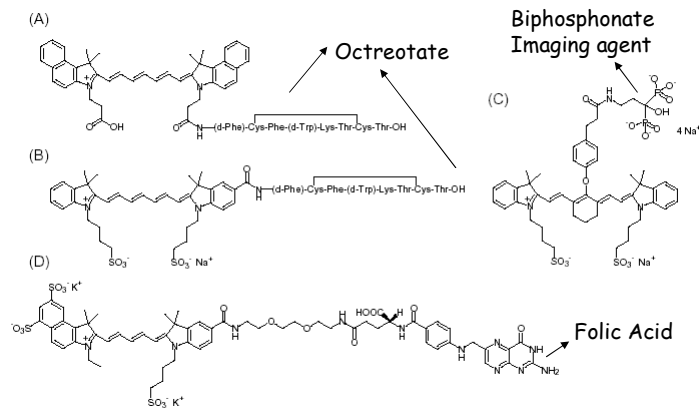
Light interaction with living tissues



Exogeneous Optical Imaging Probes:

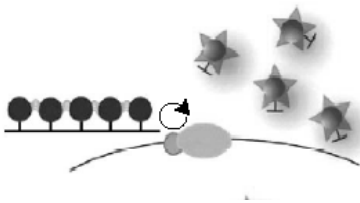
Dye conjugates for Molecular Targeting

(Ab, FAb, peptides, peptidomimetics...)



Exogeneous Optical Imaging Probes:

Activable Dyes

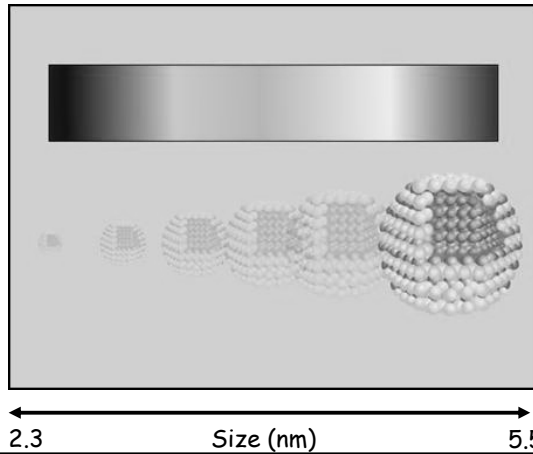


Fluorescence quenched polymeric probe:
the enzyme cleaves the peptidic poly(L-lisine) backbone
liberating dye-loaded active fragments

Exogeneous Optical Imaging Probes:

Quantum Dots

Semiconductor nanocrystals consisting of atoms such as Cd, Se, Te, S and Zn covered by different organic shells (e.g. phospholipids)



Size dependent Absorption and Fluorescence

Advantages:

- emission properties superior to organic dyes
- high fluorescence quantum yields
- long decay time
- negligible photobleaching

Endogeneous Optical Imaging Probes:

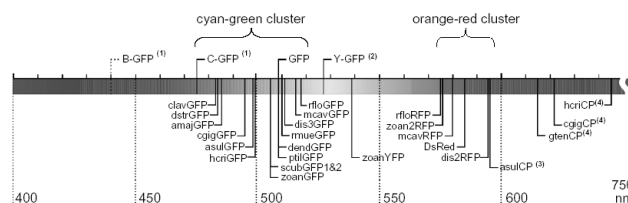
Fluorescent Proteins

Green Fluorescent Protein (GFP)



- MW= 27 KDa
- Green emitted light
- Excitation wavelength= 490 nm
- Minimal photobleaching

Emission of different GFP-like proteins



Endogeneous Optical Imaging Probes:

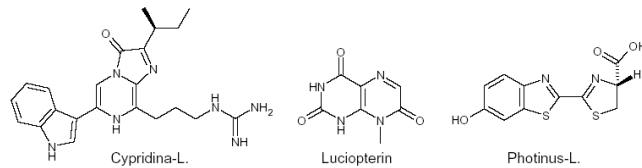
Bioluminescent Systems

Luciferase/Luciferine reporter system

Luciferases: class of oxidoreductases able to produce light when the substrate (luciferine) is present.

Ex. Firefly luciferase


Luciferin: organic compound whose oxidation in the presence of the enzyme induces bioluminescent light emission

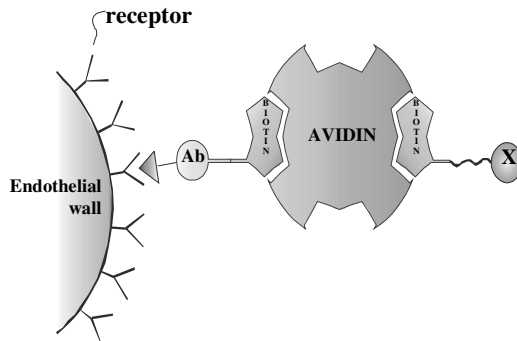


Different luciferines

Ultrasound Imaging

- Limited to vasculature

◆ **Antibody targeting**, e.g. Biotinilated antibody + Avidin +  (Y = biotine)

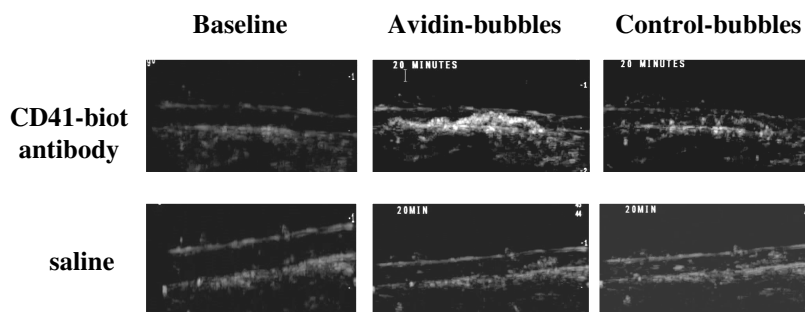


◆ **Vascular and tumor pathologies**

- ◆ Identification of specific plaques reporters
- ◆ Identification of neo-formed capillaries

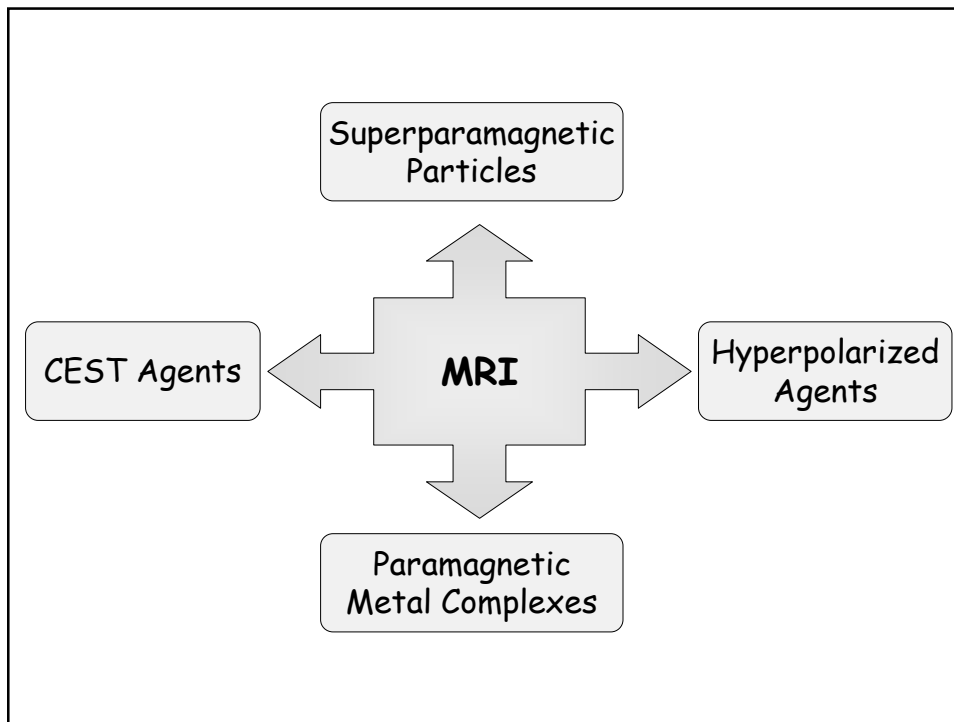
Molecular Imaging with US agents

First injection → 2nd injection → 3rd injection



- Echographic thrombus detection of avidin-conjugated microbubbles after in situ successive administration of antibody and contrast agent
- in a rabbit thrombosis model

Bracco Imaging SpA



Superparamagnetic Particles

Normally, coupling forces in ferromagnetic materials cause the magnetic moments of neighboring atoms to align, resulting in very large internal magnetic fields. When the thermal energy is sufficient to overcome the coupling forces the atomic magnetic moments can fluctuate randomly and the material exhibits paramagnetic behavior.

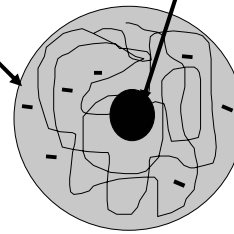
Superparamagnetism occurs when the material is composed of very small crystallites (1-10 nm).

The material behaves in a manner similar to paramagnetism, except that instead of each individual atom being independently influenced by an external magnetic field, the magnetic moment of the entire crystallite tends to align with the magnetic field.

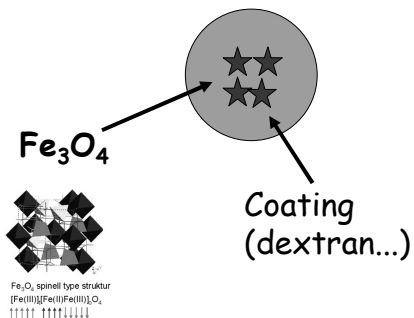
Iron Oxide Nanoparticles

Schematic view

- Iron Oxide cristal core
 - Superparamagnetic properties
- Hydrophilic Coating + charge
- Biological behavior

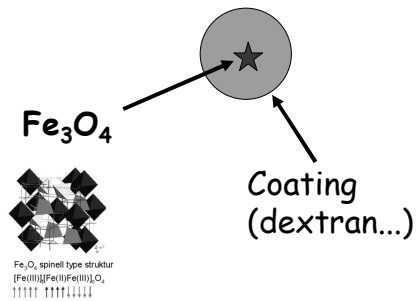


SPIO (Superparamagnetic Iron Oxides)



- Median diameter > 50 nm
 - Accumulate in the RES of the liver and spleen
 - Effective on T2 relaxation
 - Example of Commercial agent Endorem®
- Internal diameter = 4.3-4.8 nm
 Particle diameter = 200 nm
 Magnetization (25°C, 5T) = 93.6 emu/gFe
 r_1 (37°C, 20 MHz) = 24 mM⁻¹s⁻¹
 r_2 (37°C, 20 MHz) = 107 mM⁻¹s⁻¹

USPIO (Ultrasmall Superparamagnetic Iron Oxides)



- Median diameter < 50 nm
- Do not accumulate in the RES system as fast as larger particles
- longer plasma half-life
- Effective on T2 relaxation

Example of Commercial agent
Sinerem®

Internal diameter = 4.3-4.9 nm

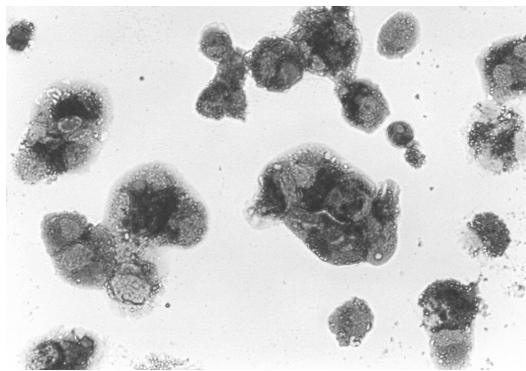
Particle diameter = 50 nm

Magnetization (25°C, 5T) = 94.8 emu/gFe

r_1 (37°C, 20 MHz) = 22.7 mM⁻¹s⁻¹

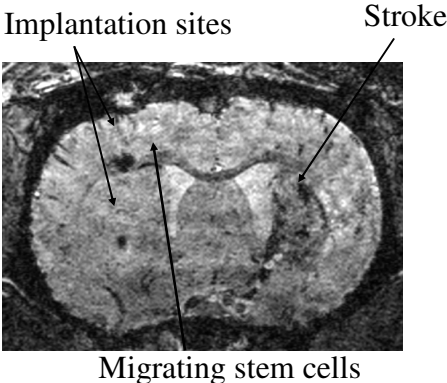
r_2 (37°C, 20 MHz) = 53.1 mM⁻¹s⁻¹

Macrophage uptake



Blue staining of iron oxide nanoparticles – Perls staining
THP-1 cells (human monocytic cell line)

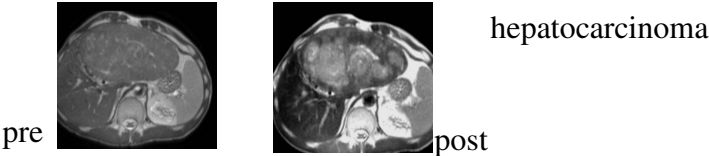
Migration of cell – Cerebral Ischemia




Hoehn M et al, Köln

Macrophage Imaging Agent LIVER Tumor Imaging

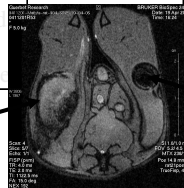
	Normal tissue	Tumor tissue	tumour
High Macrophage content in normal Tissue	Uptake of SPIO by macrophages	No uptake	normal tissue
Liver	Negative enhancement due to the T2/T2* effect of the SPIO internalized into macrophages		tumour



METASTATIC LYMPH NODE IMAGING

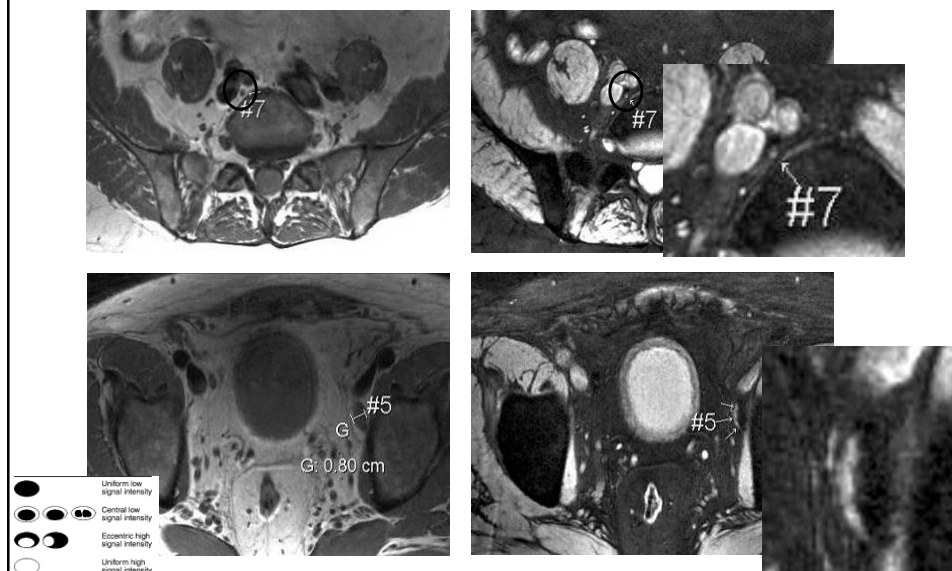
	Blood half-life	Normal tissue	Metastases	Contrast	Human Applications
MACROPHAGE IMAGING High Macrophage content in normal Lymph node	USPIO with $T_{1/2} > 6$ H are necessary to avoid major liver and spleen uptake for lymph node accumulation	Uptake of USPIO by macrophages Negative enhancement of normal tissue due to the T_2/T_2^* effect of the USPIO internalized into macrophages	No uptake due to the absence of macrophages	normal tissue  tumour	Metastatic lymph nodes (Prostate, Uterine Head and Neck, Breast, Kidney, Rectum..)

Metastatic



Normal

High Resolution MRI Small or Partially invaded Lymph nodes



Folate targeted USPIO for tumor overexpressing Folate Receptor

Choi et coll.
Acad Radiol 2004

- USPIO-folate
- In vitro : KB Cells vs A549 (FBP-)
 - In vitro proof of concept
 - ΔSI=-30% at 2.5h
- In vivo :
 - Only one mouse !
 - dose :1000 μmolFe/kg

Table 1
Uptakes of FITC-IO and Folate-FITC-IO into KB Cells and A-549 Cells Measured by Flow Cytometry

Cells	Nanoparticle	% Gated Uptake
KB	None	0.2 ± 0.0
KB	FITC-IO	6.3 ± 1.0
KB	Folate-FITC-IO	97.5 ± 0.2
A549	Folate-FITC-IO	17.4 ± 0.6

NOTE.—Values shown represent the mean ± SD (n = 2). FITC = fluorescein isothiocyanate; IO = iron oxide.

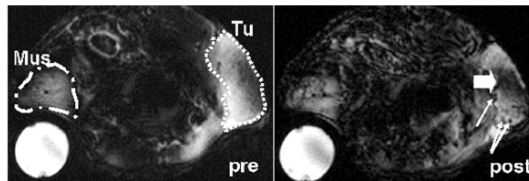


Figure 7. T2-weighted images before and 2.5 hour after intravenous administration of folate-IO nanoparticles. The two images, representative of four transverse slices from one animal, were from exactly the same slice location. Tu, tumor; Mus, muscle.

Paramagnetic Metal Complexes (Mn^{2+} , Mn^{3+} , Fe^{3+} , Gd^{3+})

La|Ce|Pr|Nd|Pm|Sm|Eu|Gd|Tb|Dy|Ho|Er|Tm|Yb|Lu



7 unpaired electrons symmetrically distributed (S-electronic state)

Very long electronic
relaxation times



High relaxing efficacy
(use as contrast agent)

- Chemically stable and easily stored in suitable form for the clinical administration
- Non-reactive in vivo and safe at diagnostic doses
- Quickly excreted
- High efficacy in altering the relaxation rates of water protons
- Endowed with targeting capability

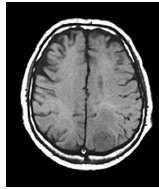
Extracellular Gd(III)-based agents in the clinical practice

[GdDTPA]²⁻ (Magnevist®)

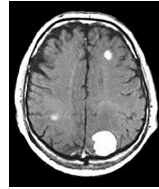
[GdDOTA]⁻ (Dotarem®)

[GdDTPA-BMA] (Omniscan®)

[GdHPDO3A] (ProHance®)



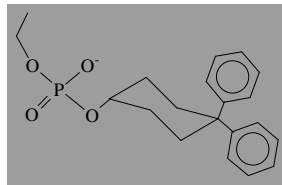
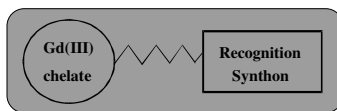
Without CA



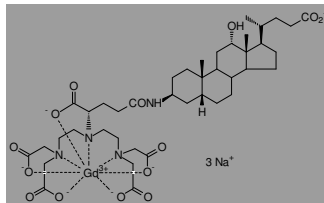
With Gd(III)-based CA

Magnetic Resonance Angiography (MRA)

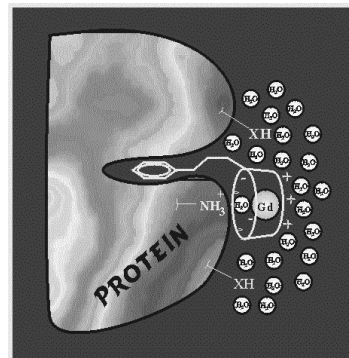
The mechanism of action of angiographic CAs is based on their interaction with human serum albumin



MS-325 (Epix)



B22956/1



Magnetic Resonance Angiography (MRA)

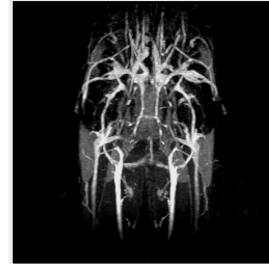
rat head (2 T)



without CA

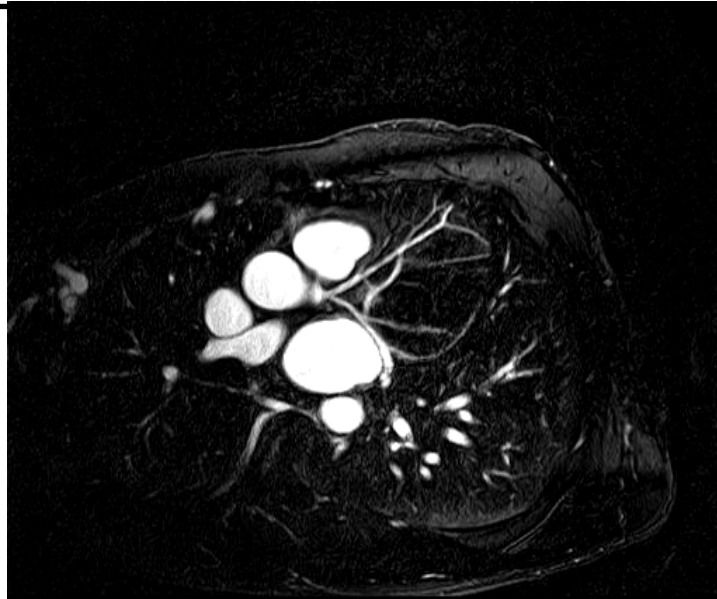


5 min. after
i.v. administration
of extracellular CA



5 min. after
i.v. administration
of angiographic CA

Blood pool agent MRI coronary angiography



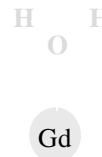
Imaging SpA

Lenghtening τ_R value ...

In order to improve the motional coupling, the metal ion has to lie at the baricentre of the molecular complex

$$\text{MW} = 1804$$

$$r_{1p}^{20} = 14 \text{ mM}^{-1} \text{ s}^{-1}$$

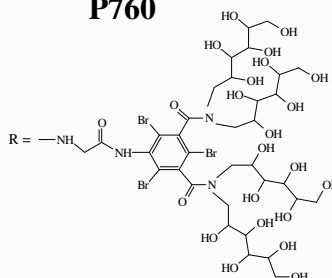
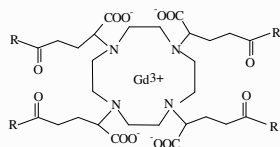


$$\text{MW} = 3100$$

$$r_{1p}^{20} = 19.6 \text{ mM}^{-1} \text{ s}^{-1}$$

D. Parker, S. Aime, et al., *Chem. Comm.* **2005**, 474-476

P760



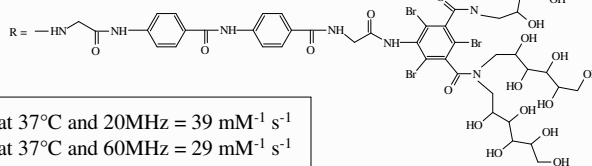
$$\tau_R = 2 \text{ ns at } 310 \text{ K}$$

$$\tau_M = 100 \text{ ns at } 310 \text{ K}$$

$$r_{1p} = 24.8 \text{ mM}^{-1} \text{ s}^{-1}$$

at 37°C and 20MHz

P792



$$r_{1p} \text{ at } 37^\circ\text{C and } 20\text{MHz} = 39 \text{ mM}^{-1} \text{ s}^{-1}$$

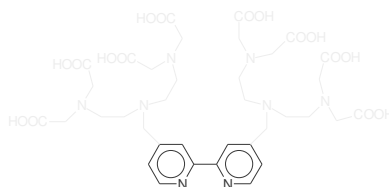
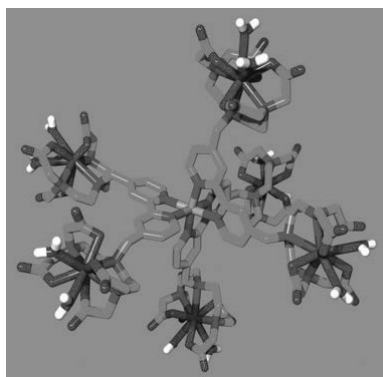
$$r_{1p} \text{ at } 37^\circ\text{C and } 60\text{MHz} = 29 \text{ mM}^{-1} \text{ s}^{-1}$$

Vander Elst, L. et al., *Eur. J. Inorg. Chem.*, **13**, 2495, 2003.

Vander Elst, L. et al., *Eur. J. Inorg. Chem.*, **6**, 1142, 2005

High Relaxivity Confined to a Small Molecular Space: A Metallostar-Based, Potential MRI Contrast Agent

João Bruno Livramento, Éva Tóth, Angélique Sour, Alain Borel, André E. Merbach, Robert Ruloff.

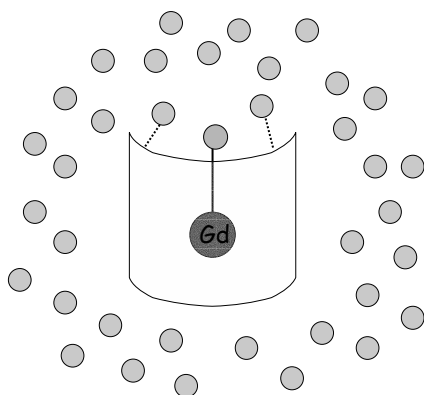


$$r_{1p} = 33.6 \text{ s}^{-1}\text{mM}^{-1} \text{ at } 40 \text{ MHz}$$

$$\text{MW} = 3744 \text{ Da}, q = 2$$

Angew. Chem. Int. Ed. **2005**, *44*, 1480-1484

Exploiting the second coordination sphere contribution....

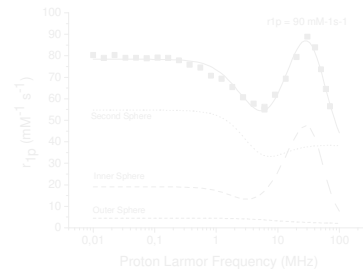
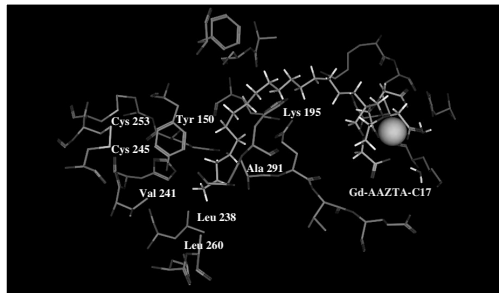


- Inner sphere water molecule
- Second sphere water molecule
- Outer sphere water molecule

$$r_1^{obs} = r_1^{inner-sphere} + r_1^{2nd-sphere} + r_1^{outer-sphere}$$

The amplification of the "2nd coord-sphere" term *via* the formation of supramolecular adducts

Gd-AAZTAC17 bound to HSA



Ca. 40% of the r_{1p}^b is given by 2nd coord. sphere contribution

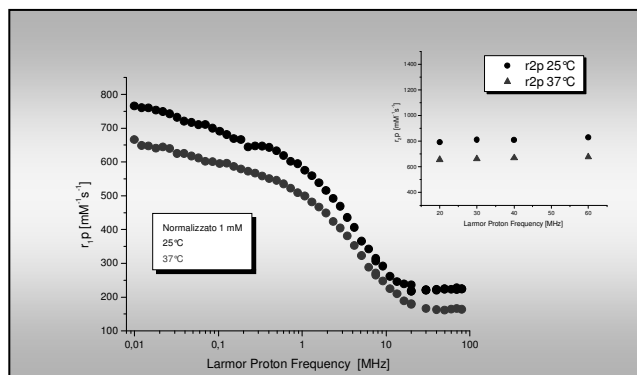
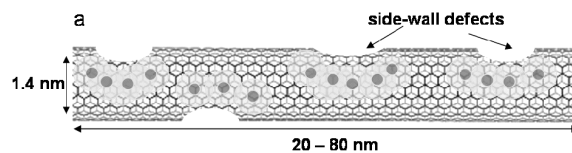
How to enhance the relaxivity of Gd(III) complexes?

New Structures with $q=2$

Are there other routes for high relaxivity systems?

Gd-Loaded Single Wall Carbon Nanotubes

Wilson LJ et al., Superparamagnetic gadonanotubes are high-performance MRI contrast agents, *Chem. Commun.*, 31, 3915, 2005.

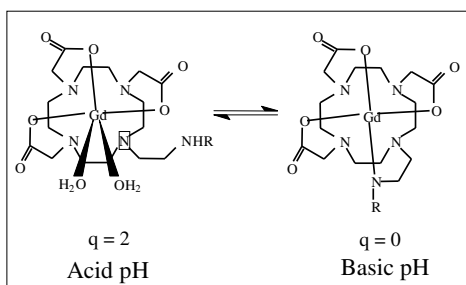


Responsive (“Smart”) Contrast Agents

Relaxivity may be made dependent on a specific parameter of the microenvironment in which the CA distributes such as:

- pH
- Temperature
- Metabolite concentration
- Enzymatic Activity

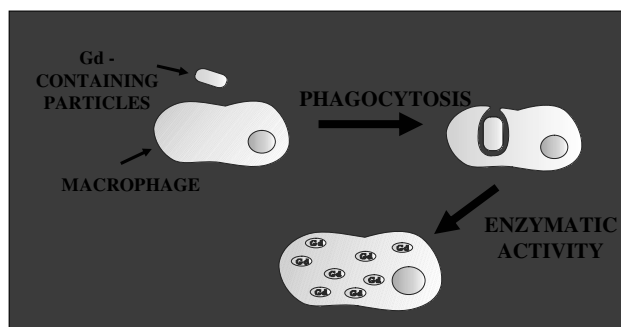
Responsive Agents: pH



Lowé MP, Parker D., Aime S, et al, JACS, 123 (31): 7601-7609, 2001

Responsive Agents: Enzymatic Activity

Insoluble Gd-chelate particulate



Intracellular Enzymatic cleavage:

INSOLUBLE

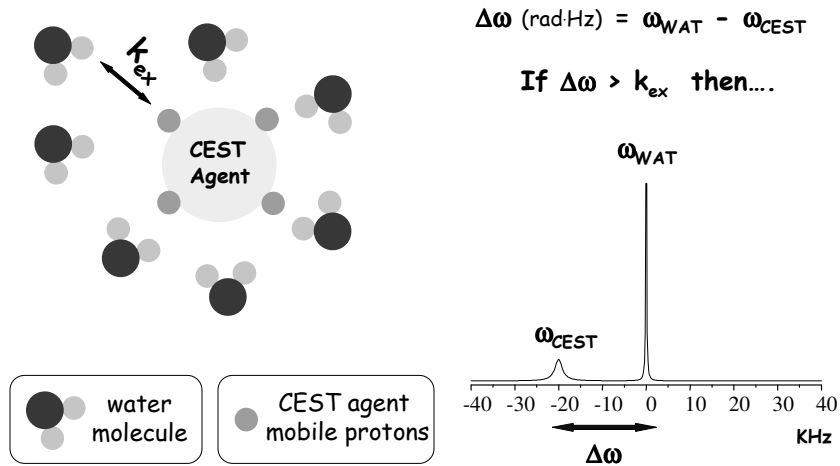


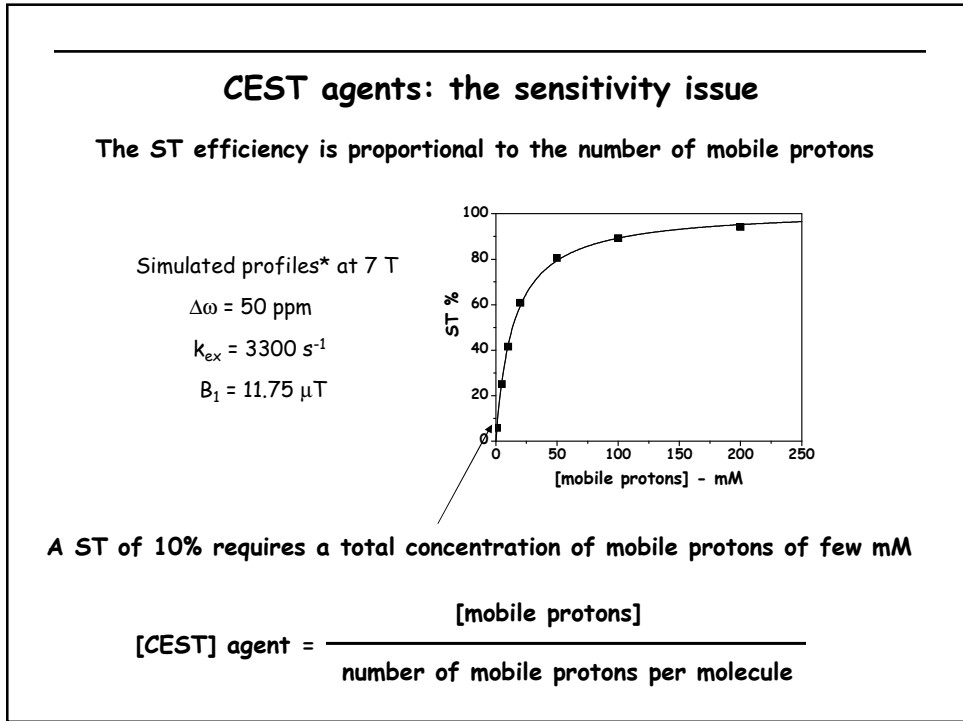
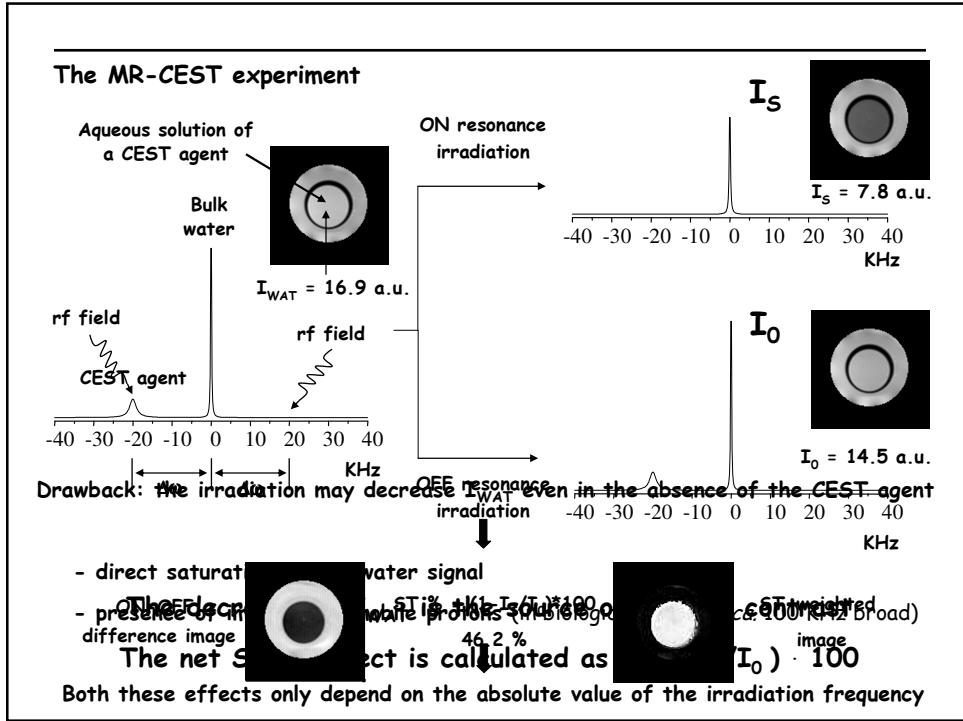
SOLUBLE

Innovative Imaging Probes

- CEST agents
- Hyperpolarized molecules

CEST (Chemical Exchange Saturation Transfer) agents

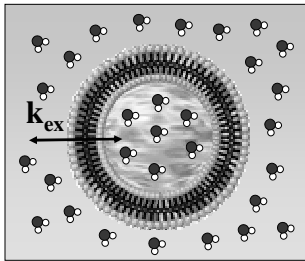




How to increase the number of mobile protons ?



Use of nanoparticles —→ Liposomes



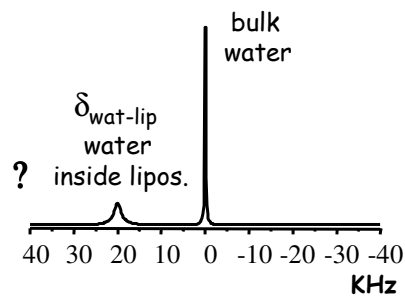
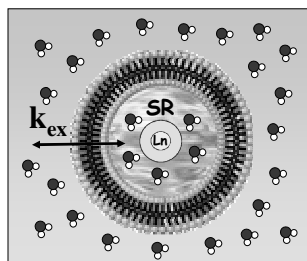
- well-known biocompatible systems
- a liposome with 200 nm of diameter contains about 2.4×10^8 mobile water protons!
- k_{ex} values cover a wide range (10 - 10^6 s^{-1}) depending on the chemical composition of the liposome membrane



In order to act as CEST agent, the resonance frequency of the water protons inside the liposome must be shifted

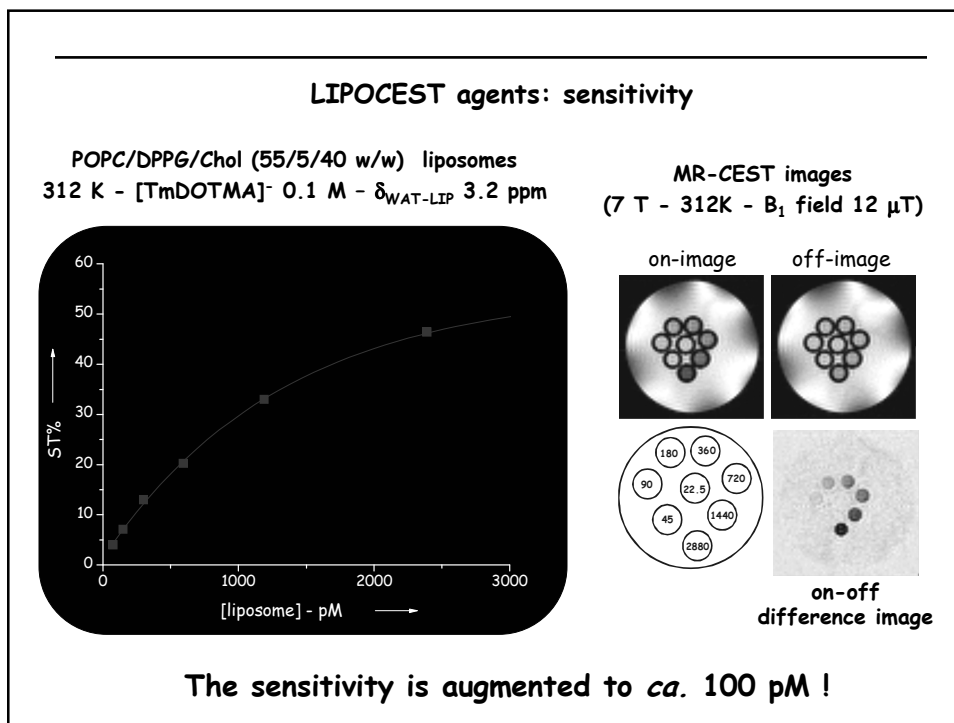
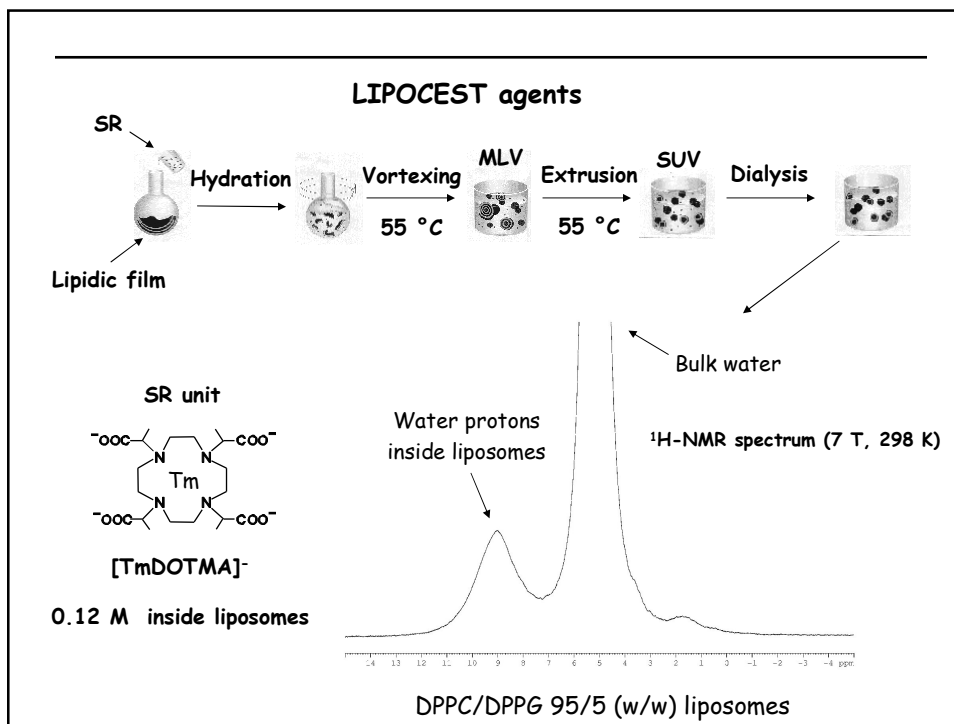
LIPOCEST agents: a new entry for highly-sensitive CEST probes

The encapsulation of a paramagnetic shift reagent (SR) in liposomes affects the resonance frequency of the water protons inside the vesicle



$\delta_{wat-lip}$ depends on the type and concentration of SR

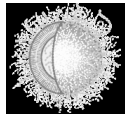
k_{ex} depends on the membrane composition and liposome size



LIPOCEST agents: passive tumor targeting in mice

Liposomes can passively target tumors by exploiting the increased vascular permeability and the lack of an efficient lymphatic drainage

But in order to prevent opsonisation processes and prolong blood lifetimes liposomes must be protected → use of STEALTH Liposomes



STEALTH Liposomes
Liposome coated by PEG chains
($t_{1/2}$ in blood up to 3 days)

Experimental set-up

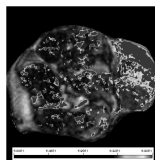
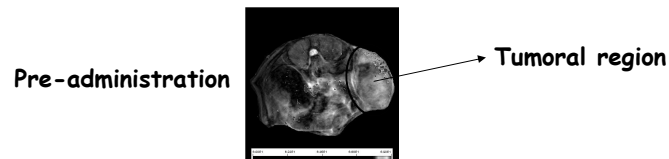
Animal model: Neuro 2A cells (murine neuroblastoma) inoculated subcutaneously to mice

STEALTH LIPOCEST: POPC/Chol/DSPE-PEG (55/40/5) liposomes
SR = [TmDOTMA]⁻ - $\delta_{\text{WAT-LIP}}$ = 2.6 ppm
diameter 110 nm

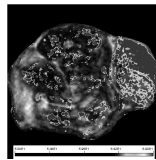
LIPOCEST agents: passive tumor targeting in mice

i.v administration of STEALTH LIPOCEST (dose: 0.04 mmol SR/kg)

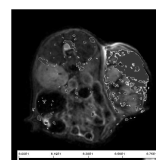
MR images at 7 T overlaid with ST-effects



3 min post



30 min post



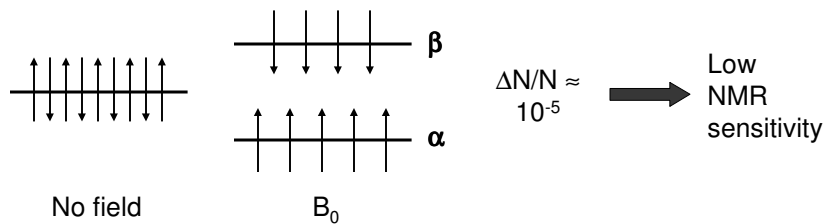
24 h post

Innovative Imaging Probes

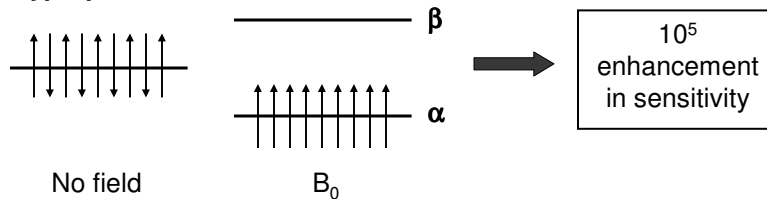
- CEST agents
- Hyperpolarized molecules

What does “hyperpolarization” mean?

◆ Normal Polarization:



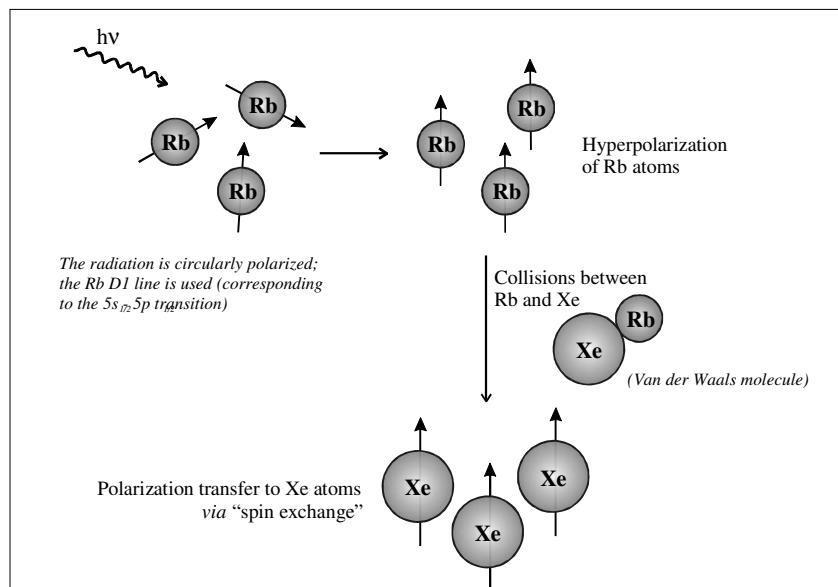
◆ Hyperpolarization:



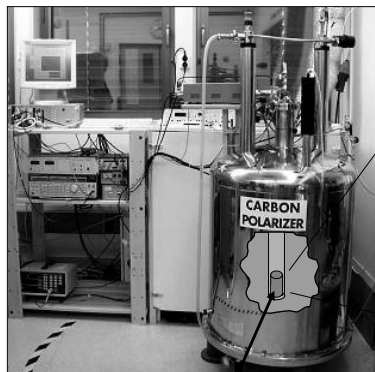
Routes to hyperpolarization

- ◆ Laser excitation (^3He or ^{129}Xe)
- ◆ “Brute Force”
- ◆ Dynamic Nuclear Polarization (DNP)
- ◆ Para-hydrogen Induced Polarization (PHIP)

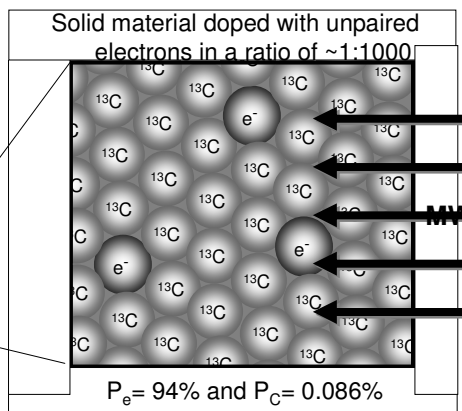
Laser-Polarized ^3He and ^{129}Xe



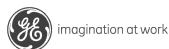
Dynamic Nuclear Polarization (DNP)



3.35 T and ~1.2K



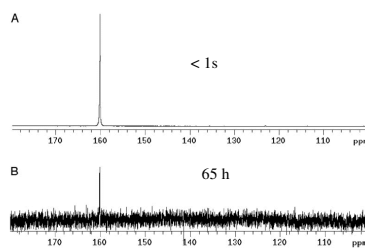
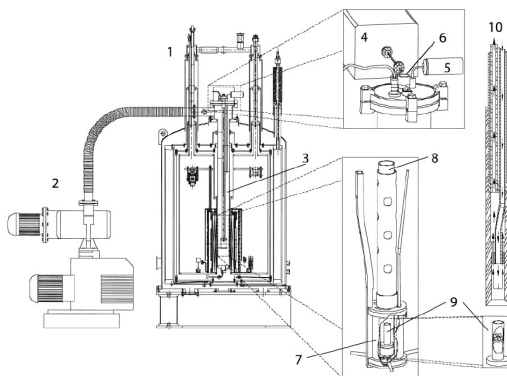
Microwaves transfer polarization from electrons to nuclei



NMR and its Holy Grail

Increase in signal-to-noise ratio of >10,000 times in liquid-state NMR

PNAS 100, 10158-10163 (September 2003)



NMR and its Holy Grail

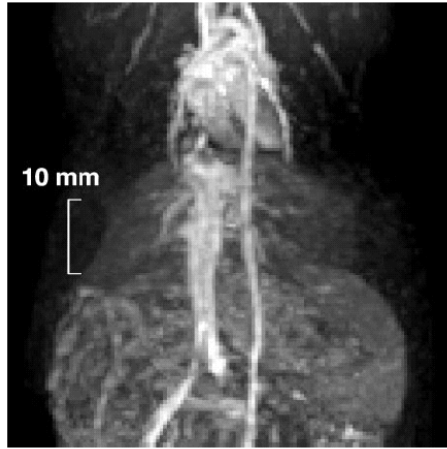
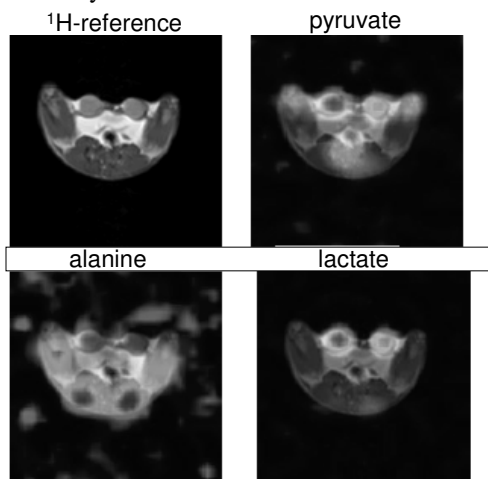


Fig. 5. A coronal MIP of a rat. The MIP was calculated from a 3D ^1H data set. The total scan time was 53 s. For other pulse-sequence parameters see *ImagIng Experiments*.

Imaging ^{13}C -labelled urea in a rat

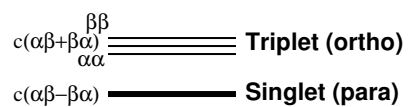
Metabolic imaging of a rat tumor with hyperpolarized ^{13}C -pyruvate

- R3230AC, mammary adenocarcinoma



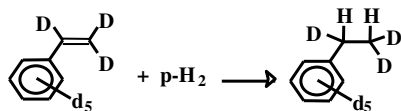
Para-hydrogen Induced Polarization (PHIP)

What Para-Hydrogen is?

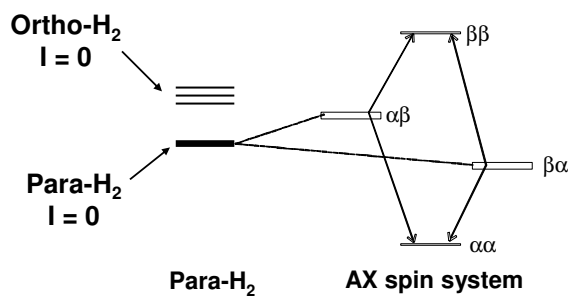
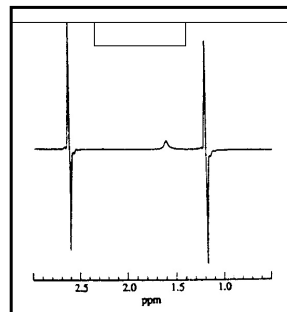


Normal Hydrogen =
75% ortho + 25% para

Para-Hydrogen Induced Polarization (PHIP)



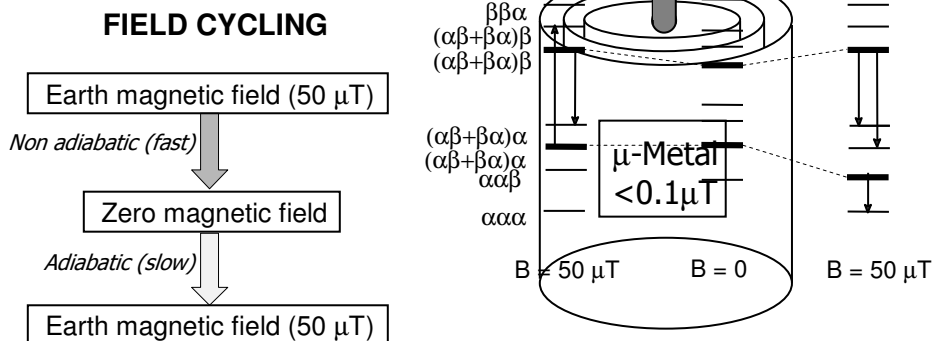
Resulting ^1H NMR spectrum:



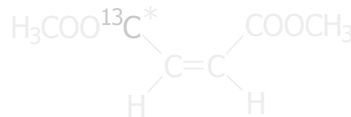
**Signal enhancement
up to 10^5**

Para-H₂ containing molecules as hyperpolarized contrast agents

In order to obtain a ¹³C image by using the ¹³C polarized signal, it must be transformed from antiphase to in-phase



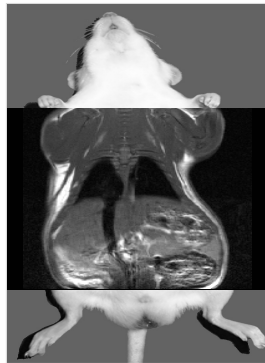
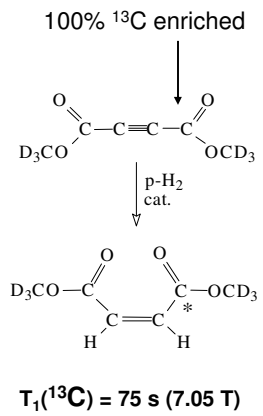
FIELD CYCLING - effect upon the ¹³C polarized signal of



Field cycling ↓

**The Nycomed approach:
Para-H₂ containing molecules as hyperpolarized C.A.**

Sub-second ¹³C-angiography

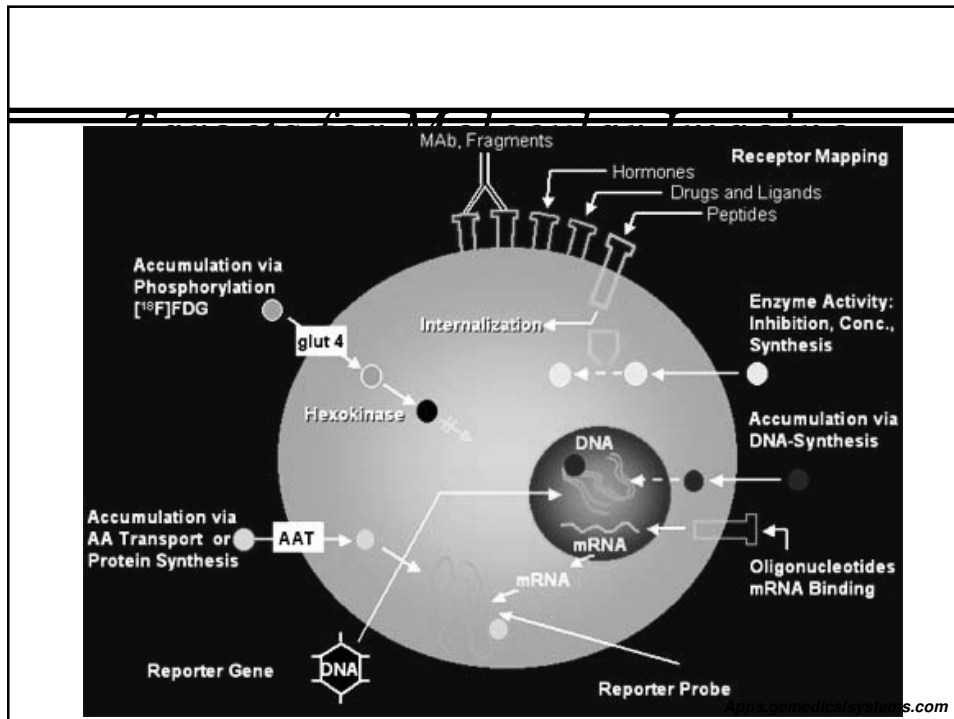


normal spin echo (SE) image (¹H)



single shot RARE sequence (¹³C)

Magn. Res. In Med., 2001, 46, 1



Acknowledgements

University of Torino:

Dept. of Chemistry

E. Terreno
S. Geninatti Crich
A. Barge
E. Gianolio
D. Delli Castelli
L. Tei
D. Longo
A. Viale
W. Dastrù

Bioindustry Park Canavese

C. Cabella
F. Fedeli
G. Digilio
A. Mortillaro

University of Eastern Piedmont

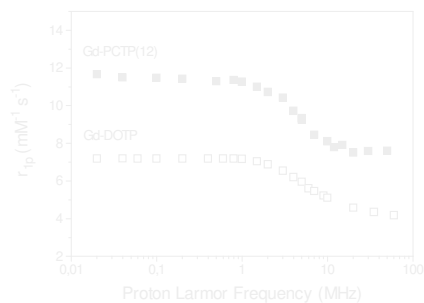
M. Botta (Alessandria)
G.B. Giovenzana (Novara)
C. Cavallotti (Novara)

Bracco Imaging SpA (Milano)

F. Uggeri
P.L. Anelli
M. Fumagalli
L. Lattuada
V. Lorusso

The second coordination sphere contribution:

$\text{Gd-DOTP} \rightarrow q = 0$ only 2nd and outer sphere
 $\text{Gd-PCTP(12)} \rightarrow q = 1$ + 2nd sphere contribution



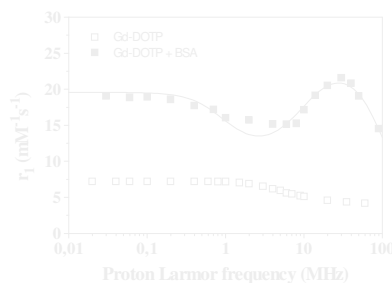
The amplification of the "2nd coord-sphere" term *via* the formation of supramolecular adducts

Gd-DOTP bound to BSA



The NMRD profile is rather similar both in shape and amplitude to those measured for $\varphi=1$ complexes

Aime, S.; Botta, M.; Fasano, M.; Geninatti Crich, S.; Terreno, E. *J. Biol. Inorg. Chem.*, **1996**, 1, 312-319.



CEST agents: the sensitivity issue

The ST efficiency is proportional to k_{ex} ...

...but the exchange rate of the mobile protons cannot be increased at will !

i) the condition $\Delta\omega > k_{ex}$ has to be satisfied

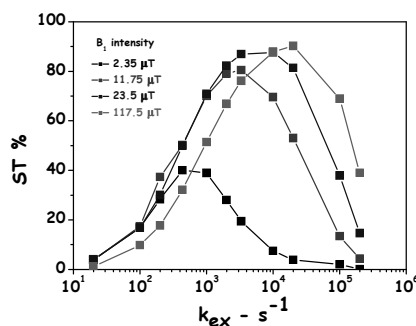
ii) high k_{ex} values require large B_1 intensity values (risk of unsafe irradiation) in order to fully saturate the mobile protons of the CEST agent

Simulated profiles* at 7 T

$\Delta\omega = 50$ ppm

[mobile protons] = 50 mM

At maximum ST % $\rightarrow \frac{k_{ex}}{B_1} = 2\pi$



* D.E. Woessner et al., *Magn. Res. Med.*, **2005**, 53, 790

Small-sized molecules → small number of mobile protons (2-8) per molecule

◆ Diamagnetic agents

Sugars, aminoacids, heterocyclic compounds, nucleosides

R. Balaban et al., *J. Magn. Res.*, 2000, 143, 79.

◆ Paramagnetic agents

Lanthanide-based metal chelates (PARACEST)

A.D. Sherry et al., *J. Am. Chem. Soc.*, 2001, 123, 1517.

S. Aime et al., *Magn. Res. Med.*, 2002, 47, 639.

sensitivity in
the mM range

Macromolecular agents → higher number of mobile protons (~10³) per molecule

◆ Diamagnetic agents

Polyaminoacids, dendrimers, RNA-like polymers, ...

P.C.M Van Zijl et al., *Magn. Res. Med.*, 2003, 49, 998.

◆ Paramagnetic agents

Supramolecular adducts (SUPRACEST)

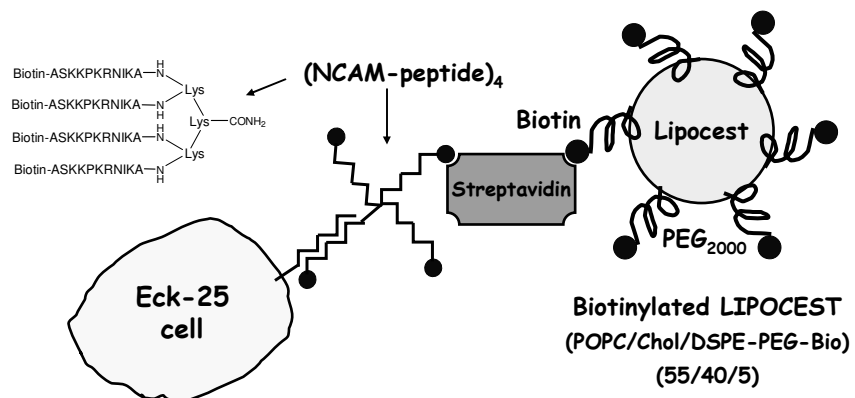
S. Aime et al., *Angew. Chemie Int. Ed.*, 2003, 42, 4527.

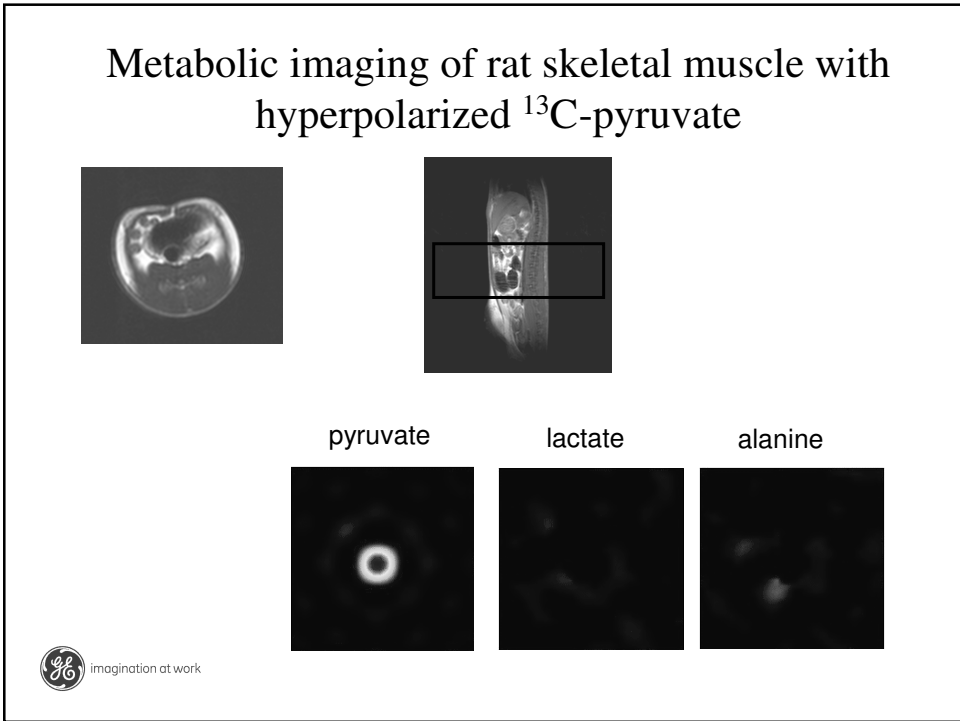
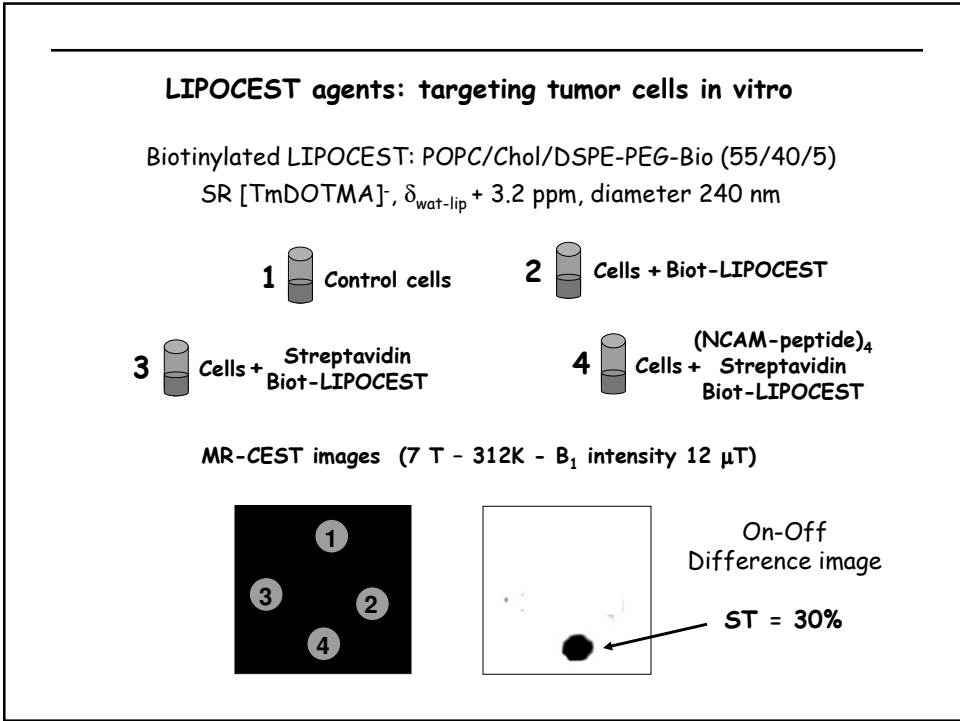
sensitivity in
the μM range

LIPOCEST agents: targeting tumor cells *in vitro*

Cellular model: Eck-25 cells

Immortalised microendothelial cells derived from a human renal carcinoma
overexpressing the Neural Cell Adhesion Molecule (NCAM)





Production of ^{13}C -labelled lactate from ^{13}C labelled pyruvate in an EL4 lymphoma cell suspension

